New Journal of Chemistry

In-situ analysis of pesticide residues on the surface of agricultural products via surface-enhanced Raman spectroscopy using a flexible Au@Ag-PDMS substrate

Hang Zhao,[a] Wuliji Hasi,*[a] Nan Li,[a] Xuanyu Sha,[a] Shuang Lin,[a] Siqingaowa Han[a, b]

a. National Key Laboratory of Science and Technology on Tunable Laser, Harbin Institute of Technology, Harbin, Heilongjiang 150080, China. E-mail: hasiwuliji@126.com

b. Affiliated Hospital of Inner Mongolia University for the Nationalities, Tongliao, Inner Mongolia 028007, China

List of supplementary material

SI-1 PDMS pretreatment and wafer substrate preparation

First, the PDMS stock solution and the curing agent were mixed at a ratio of 10:1, thoroughly stirred, and then degassed in a vacuum chamber for 30 min to completely degas. Each 5 g PDMS premix is spread by a spin coater and horizontally placed in a constant temperature oven at 60 °C for 2 h. Finally, the film was peeled and cut into squares with a side length of 10 mm. Clean silicon wafers were immersed in hydrophilic treatment fluid (ammonia, hydrogen peroxide: water = 1:1:5 v/v), heated 30 minutes at 90 ℃. After being removed, it was rinsed with ultra-pure water and treated with ultrasound for 30 minutes.

SI-2 Effects of imazilil on the morphology of nanoparticles

Au@Ag nanocubes were assembled onto silicon wafers and divided into two groups. SEM was taken directly in group A, and soaked in imazilil solution with 5 mg L^{-1} concentration for 5 min in group B. After that, they were taken out and dried for SEM. The results showed that there was no obvious difference between the two substrates in SEM images. The morphology and structure of imazilil molecules were not significantly changed on the surface of the cube.

SI-3 Influence of PH value on SERS detection process

In the experiment, hydrochloric acid and sodium hydroxide were used to adjust the PH of 4-MBA solution to 3.69 and 12, and then their signals were collected through the Au@Ag-PDMS substrate, and it was found that, compared with the neutral condition (PH=6.83), the SERS spectral strength of 4-MBA under acidic condition decreased significantly, while the spectral strength increased under alkaline condition. According to the literature, this is due to the different adsorption behaviors of 4-mba on the surface of nanoparticles. However, the actual detection of pesticide residues, especially in situ detection, is generally conducted under neutral conditions, which is conducive to the identification by comparison with the standard spectrum. Under acidic and alkaline conditions, the adsorption state and even molecular structure of the molecules to be tested may be changed, resulting in the change of SERS spectrum.

SI-4 Conversion of maximum pesticide residues to detectable concentrations

Assuming that the drug remains uniformly on the surface of the apple, the relationship between the measured concentration of the drug on the sample C_α and the drug residue φ across the apple is established:

$m_s = \bar{P}_s \times S_s \times H_t$

$m_t = \bar{P}_t \times S_t \times H_t$

$\bar{P}_s = \bar{P}_t$

$$m_\alpha = C_\alpha \times V_\alpha \times \frac{S_t}{S_s} = C_\alpha \times V_\alpha \times \frac{m_t}{m_s}$$

$$\varphi = \frac{m_\alpha}{m_\beta} = \frac{V_\alpha \times m_t}{m_\beta \times m_s} C_\alpha$$

Where m_β represents the total mass of the remaining apple. H_t represents the thickness of the cut apple skin, m_t represents the mass of the entire apple epidermis, S_t represents the area of the entire apple epidermis, and $\bar{P}_t$ represents the average density of the cut epidermis. S_s represents the area of the apple skin sample, generally taking a unit area of 1 cm^2, m_s represents the mass of the skin sample, and $\bar{P}_s$ represents the average density of the skin sample. m_α represents the mass of the drug on the whole apple, and V_α represents the volume of the pure solvent added to the sample. φ represents the mass fraction of drug residues on the entire apple, C_α represents the detected concentration by SERS.

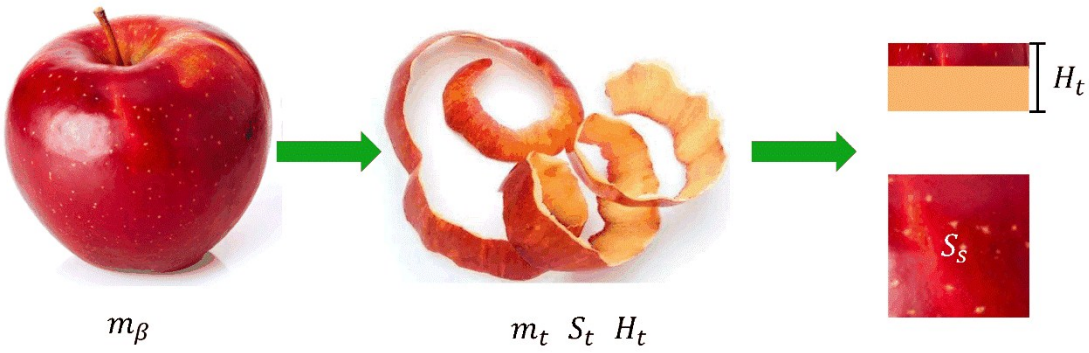

Fig.S1 Schematic diagram of apple skin treatment

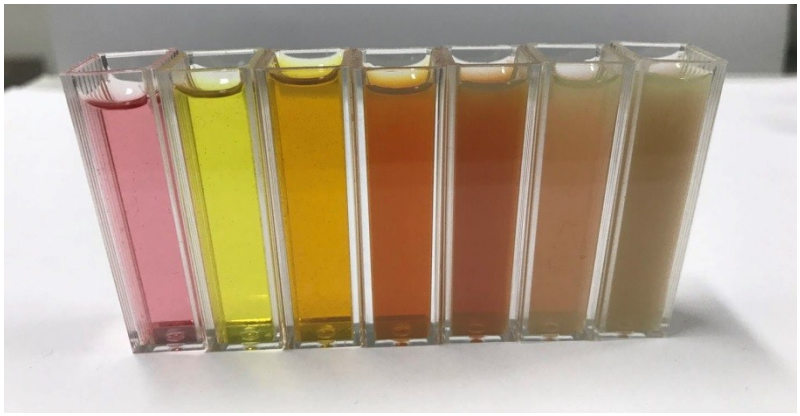

Fig. S2 Photos of silver and gold nanocubes.The side length of the cube increases from left to right

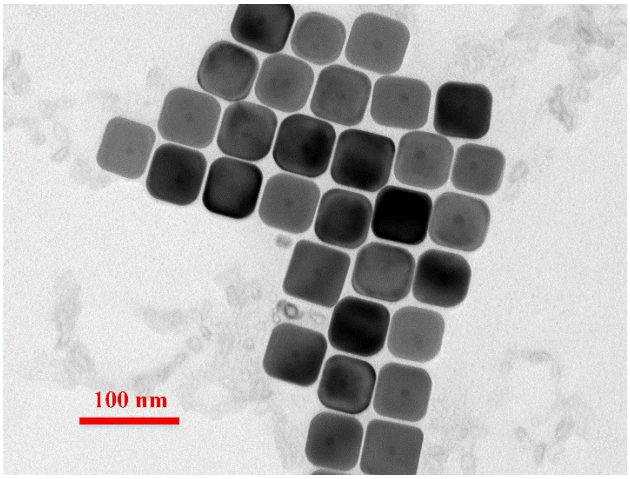

Fig. S3 Transmission electron microscope image of 51.65 nm silver-coated gold nanocube

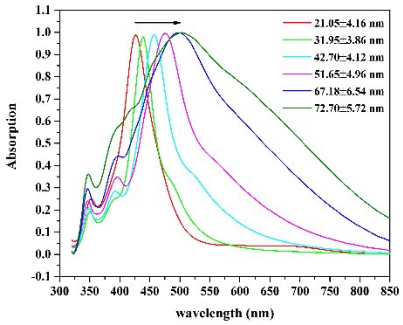

Fig. S4 UV-visible absorption spectra corresponding to Au@Ag nanocubes

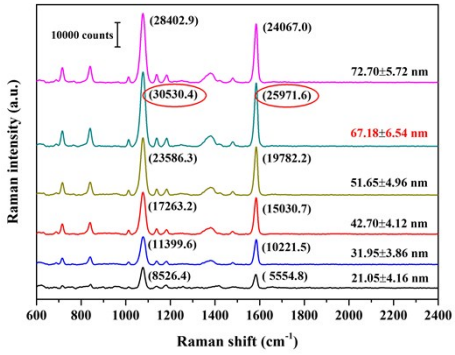

Fig. S5 Detection spectra of different particle size on nanocube substrates on the same concentration of 4-MBA (10^{-6} M). Obviously, the nanoparticles with 67.18±6.54 nm side length have the best enhancement effect.

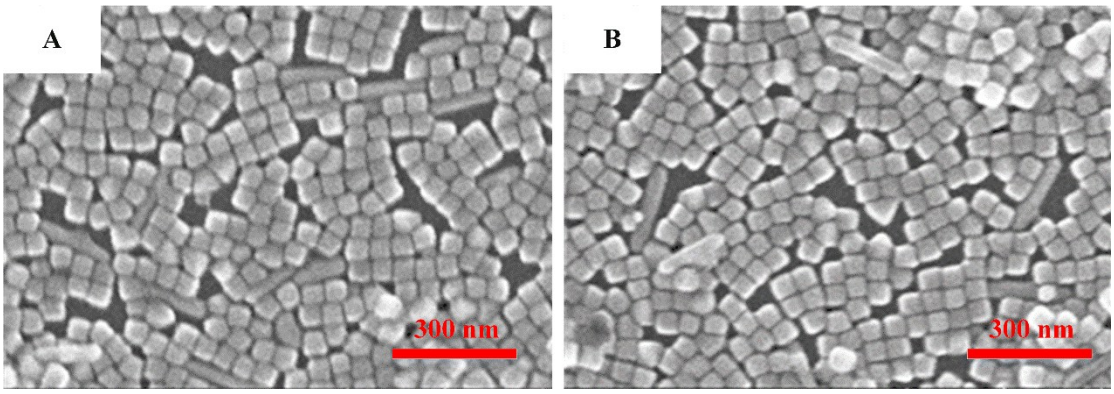

Fig. S6 SEM images before (A) and after (B) immersion with imazilil

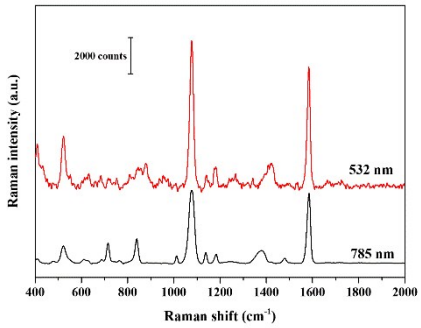

Fig. S7 Au@Ag-PDMS substrate was excited by 532 nm and 785 nm light sources respectively to detect 10^{-6} M of 4-MBA

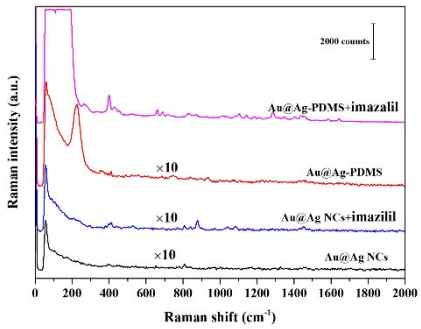

Fig. S8 Blank spectra of Au@Ag NCs (black line) and Au@Ag-PDMS substrate (red line). SERS spectrum of Au@Ag NCs (blue line) with equal volume 10 mg/L imazilil. SERS spectrum of Au@Ag-PDMS substrate after dropping imazilil (pink line).

Table S1 The location of Raman characteristic peak and its possible attribution

Solid /cm^{-1}	Calc. /cm^{-1}	SERS /cm^{-1}	Vibrational Assignment
190	205	192	$\delta R_1+\delta(C_{11}\text{-}H)$
278	293	278	$\delta(O_6\text{-}C_{11}\text{-}C_{15}=C_{19})+\delta R_2$
327	326	327	$\delta R_1+\delta R_2+\delta(C_2\text{-}O_6\text{-}C_{11})$
367	357	364	$\delta(C_5\text{-}N1_0\text{-}C_{13})$
397	401	399	$\delta(C_7\text{-}C_{12}\text{-}C_9)+\delta(C_2\text{-}O_6)+\delta(C_5\text{-}H)$
410	405	-	$\delta(R_1\text{-}C_5\text{-}C_2)$
452	472	457	$\delta(O_6\text{-}C_{11})+\delta(C_3\text{-}C_1=C_4)+\delta(C_{15}=C_{19})$
528	535	528	$\delta(C_1=C_4\text{-}C_9)+\delta(C_5\text{-}C_2\text{-}O_6)$
628	588	630	$\delta R_1+\delta(C_1\text{-}C_2\text{-}C_5)$
637	634	-	$\delta R_2+\delta(C_{19}\text{-}H)$
658	660	661	$\delta(C_6\text{-}C1_1\text{-}C1_5)+\delta(C_1=C_4)$
687	673	689	$\delta(C_{14}=N_{18}\text{-}C_{17})+\delta(C_2\text{-}C_5+R_1)$
690	703	-	$\delta R_1+\delta(C_2\text{-}C_5)$
718	729	720	$\delta(C_{13}\text{-}H)+\delta(C_{14}\text{-}H)+\delta(C_{17}\text{-}H)$
754	755	752	$\delta(C_{13}\text{-}N_{10}\text{-}C1_5)+\delta(C_{11}\text{-}O_6)$
833	827	830	$\delta(C_4\text{-}H)+\delta(C_5\text{-}H)+\delta(C_9\text{-}H)$
845	836	841	$\delta R_1+\delta(C_2\text{-}C_5)$
869	865	873	$\delta(N_{18}\text{-}C1_7=C_{13})$
918	920	914	$\delta(O_6\text{-}C_{11}\text{-}C_{15})+\delta(C_{19}\text{-}H)$
971	978	973	$\delta(C_5\text{-}C_2\text{-}O_6\text{-}C_{11})+\delta(C_{15}\text{-}H)+\delta(C_{19}\text{-}H)$
1011	1019	1011	$\delta(C_{15}\text{-}H)+\delta(C_{19}\text{-}H)$
1027	1043	1029	δR_2
1038	1058	1042	$\delta(C_4\text{-}C_9)+\delta(C_3=C_7)+\delta(C_2\text{-}C_5)$
1073	1081	1085	$\nu(C_3\text{-}C_1=C_4)+\delta(C_2\text{-}C_5)$
1099	1100	1091	$\nu(C_{13}=C_{17})$
1105	1104	1104	$\nu(C_2\text{-}O_6\text{-}C_{11})+\delta(C_9\text{-}H)+\delta(C_{13}\text{-}H)+\delta(C_{17}\text{-}H)$
1142	1144	1142	$\nu(C_{17}\text{-}N_{18})$
1185	1196	1186	$\delta(C_{11}\text{-}C_{15}=C_{19})+\delta(C_5\text{-}C_{10}\text{-}C_{14})$
1212	1215	1214	$\nu(C_1\text{-}C_2)+\delta R_1$
1252	1265	1252	$\delta(C_{14}=N_{18})$
1284	1281	1286	$\delta(C_4\text{-}H)+\delta(C_7\text{-}H)+\delta(C_9\text{-}H)$
1292	1294	1303	$\delta(C_2\text{-}H)+\delta(C_5\text{-}H)+\delta(C_{11}\text{-}H)$
1314	1322	-	$\delta(C_{11}\text{-}H)+\delta(C_{15}\text{-}H)+\delta(C_{19}\text{-}H$
1345	1343	1344	$\delta(C_2\text{-}C_5)+\delta(C_{11}\text{-}H)+\delta(C_{15}\text{-}H)+\delta(C_{19}\text{-}H)$
1385	1384	1386	$\delta(C_2\text{-}C_5\text{-}N_{10})$
1391	1392	-	$\delta(C_{14}=N_{18}\text{-}C_{17})+\delta(C_2\text{-}H)+\delta(C_5\text{-}H)+\delta(C_{11}\text{-}H)$
1400	1394	1405	$\delta(C_2\text{-}H)+\delta(C_5\text{-}H)+\delta(C_7\text{-}H)+\delta(C_9\text{-}H)+\delta(C_{11}\text{-}H)$
1421	1414	1421	$\delta(C_{14}\text{-}N_{10}\text{-}C_{13})+\delta(C_5\text{-}H)$
1433	1432	1437	$\delta(C_2\text{-}H)+\delta(C_5\text{-}H)+\delta(C_9\text{-}H)$
1458	1463	1457	$\delta(C_{11}\text{-}H)+\delta(C_{15}\text{-}H)+\delta(C_{19}\text{-}H)$
1502	1505	1499	$R_1+\delta(C_2\text{-}H)$
1538	1534	1526	$\delta(C_{13}\text{-}N_{10}\text{-}C_{14})+\delta(C_5\text{-}H)$
1561	1545	1558	$\delta(C_{14}=N_{18})+\delta(C_5\text{-}H)$
1588	1600	1587	$\nu(C_1\text{-}C_3)+\nu(C_9=C_{12})+\delta(C_2\text{-}H)$
1639	1630	1643	δR_1
	1711		$\nu(C_{15}=C_{19})$

Note: δ is for bending vibration and ν is for stretching vibration

Table S2 The weighing results of three experimental samples

Samples	m_{β}/g	m_{t}/g	m_{s}/g	C_{α}/mg L^{-1}
Apple	360	33	0.126	27.49φ
Citrus	192.9	27.2	0.161	22.84φ
Tomato	287	29.5	0.262	50.98φ

Note: The average weighing results of 5 samples are shown in the table

Table S3 Detection results of SERS and HPLC method on imazilil pesticide residues

	LOD^{1} mg/L	LOD^{2} mg/L	Detection time	Linear range mg/L
SERS	0.1	2	30 min	2-15
HPLC	0.005	0.04	>6h	0.05-5

Note: LOD^{1} refers to the detection of imazole standard solution and LOD^{2} to the detection of imazole residue in apples. Detection time includes the whole process of sample processing, conditional exploration and detection. SERS detection results are not compound with absolute linear relationship, so the detection range of this paper is given.